

## **Indications of an extreme event deposits along the west coast of India: evidences from GPR investigations**

Loveson, V. J\*., Gujar, A. R<sup>1</sup>., Iyer, S.D<sup>1</sup>., Srivastava, P<sup>2</sup>., Tirodkar, G.M.<sup>1</sup> and Luis, R. A. A<sup>1</sup>

\*CSIR-Central Institute of Mining & Fuel Research, Dhanbad, Jharkhand, 826001, India

<sup>1</sup>CSIR-National Institute of Oceanography, Dona Paula, Goa, 403004, India

<sup>2</sup>Wadia Institute of Himalayan Geology, Dehradun, Uttarakhand 248001

\* Corresponding Author :

email: [vjloveson@yahoo.co.uk](mailto:vjloveson@yahoo.co.uk)

Telephone: +91(326) 2206016

Mobile: +919431121459

Fax: +91(326) 2296025

### **Abstract**

The Ground-Penetrating Radar (GPR) was used to trace the subsurface details in the Palshet coastal zone (Maharashtra) as it exhibits an interesting array of geomorphological features. Furthermore, our main goal was to identify and locate features that might have formed during a reported extreme event and its effect on the flow of the nearby Sundri River. Two profiles (8 m and 4 m depth) were collected across the beach and along the backshore respectively. While the 8 m depth profile (west to east; across the beach) indicates a series of coastline regression in this area, the 4 m depth profile along the coastline (north to south) in the backshore zone reveals two significant incidents viz., i) stages of development of the paleo-channels that indicate the migration of the Sundri River towards south and ii) huge sediment deposit up to 2.5 m thick in the backshore area. The erosional relict surface (~2.5 m depth) was traced along with various spells of sediments that perhaps occurred due to an extreme event. Sand samples were collected from two trial pits along the GPR profiles to understand the sedimentology and mineralogy in the backshore area. These data together with beach profiles and geomorphological maps suggest that the sands were deposited by an extreme event perhaps during the 1854 cyclonic storm. The sands were trapped in suitable geomorphological sites along the Palshet coast and this sand deposit of about 2.5 m thickness, forced the shifting of the River Sundri towards the south. This new revelation facilitates a further study that could focus on the nearby coastal areas to document such extreme event deposits.

Keywords: GPR, *Subsurface mapping, raised beach deposits, river migration, paleo-channel, Maharashtra*

## 1.0 Introduction

The cyclonic storms are more common along the Indian coasts, which usually cause extensive damages to the coastal properties, devastate the coastal landforms and persistently claim human lives. Being one of the worst affected by severe cyclones and cyclonic storms, the Indian maritime regions (of Bay of Bengal and Arabian Sea) are intensely exposed to nearly 10% of world's tropical cyclones (Dube et al. 1997). During the pre- and post-monsoon periods, such tropical storms are more frequent in the Bay of Bengal region (an average of 5 to 6 of which 2 or 3 could be destructive) and most of which were well studied through numerical modeling (Unnikrishnan et al. 2011). But, the Arabian Sea tropical cyclogenesis is less studied than that of the Bay of Bengal (Murthy and El-Sabh 1984; Pedgley 2012), though at least 2 or 3 cyclones of various intensities are formed over the Arabian Sea each year (Evan and Camargo 2011; Rajeevan et al. 2013). However, the studies on cyclogenesis and characteristics of earlier cyclones aid to devise suitable disaster management plans which further leads to equip for preparedness to mitigate the future eventualities and minimizing the casualties and property loss. Moreover, documentation of the paleo-extreme events of yester centuries through field sedimentary records are more essential to realize the magnitude, to characterize the paleo-extreme events and to understand the relation with the present ones. But, the poor preservation of the paleo-extreme events sediment and morphological features create more complicatedness for documentation of such sedimentary records.

Above and beyond the documentation of the metrological information pertain to the cyclonic storms in Arabian Sea, the studies on morphological changes in the coastal features and characterization on sediments are rare. This is also true that the paleo-storm deposits are rarely studied and documented in sedimentological point of view. During the recent field studies (2009-2012) related to paleo-tsunami / storm mapping project along the west coast of India, based on earlier records on cyclones and present day coastal geomorphology, few coastal zones were marked for detailed study, with a objective to document extreme event sediments, among which the study area the Palshet coast is one.

The GPR studies on the alluvial plain to understand the internal architecture of sedimentary bed sets, to trace paleo-channels and to reconstruct fluvial dynamics are well known (Vandenberghe and van Overmeeren 1999; Neal et al. 2002; Gourry et al. 2003; Sridhar and Patidar 2005; Smith et al. 2006; Smith et al. 2009; Slowik 2011; Altdorff et al. 2013). Maksim (2000) studied the water table characteristics, channels and meander bar from their significant reflection using 100 MHz antenna and correlated with borehole and trench data. Slowik (2012) deliberated the influence on the depth range and resolution of GPR under three different sets of hydrological condition in valley

alluvial fill area with reference to various groundwater table conditions and frozen flood plan. Patidar et al. (2007) used GPR along with other field data to trace the nature of fault extension in Quaternary alluvial sediments for understanding the tectonic activity in the contemporary setting. In addition, the GPR ability in mapping the characteristics and internal sedimentary architecture of extreme event deposits were established by various earlier studies (Neal 2002; Loveson et al. 2005; Loveson and Gujar 2010; Shukla 2012; Koster, 2012; Loveson et al. 2014).

The main goals of the present study were to investigate the sedimentary record of extreme events in beach deposits and the influence of this event on the shifting course (avulsion) of the Sundri River. Our approach is based on a non-destructive geophysical method to obtain a near-continuous record of the subsurface sedimentary pattern and its correlation with the field observation from trial pits. Since the present GPR study was conducted in the coastal zone, the essential limiting factors include i) salinity character of the subsurface (sea water saturation) where signal attenuation was recorded below ~2 to 4 m depth and ii) a low to elevated study area (~0 to 8 m mean sea level) where the low-frequency noise of the ground was encountered. Optically stimulated luminescence (OSL) dating was also carried out to decipher the time of the extreme event which led to a huge deposition of sand.

## **2.0 Study area**

The Palshet ( $17^{\circ} 26'31''$  N and  $73^{\circ} 11'43''$  E) coastal zone of central Maharashtra (Fig. 1a) was chosen for this present study. The Palshet beach is about 2 km long and nearly 250 m wide. It is an arcuate bay beach with promontories on the either sides (Fig. 1b). The beach is moderately steep with an elevated berm and a wide backshore area. The inter-tidal zone is steep. The elevated berm and backshore areas are almost barren and the topography is rugged (Fig 2 a). An unusual occurrence is the accumulation of lateritic pebbles and coarse sand along with heavy minerals to a height of nearly 4 m in the berm area as a raised beach ridge. This accumulated debris could have deposited during an unusual process like a storm / cyclone / tsunami. We investigated this feature to understand the depositional processes involved in its formation. The northern side lateritic promontory shows sharp and broken boulders at the water level. Beyond the berm the coast is a low lying terrain with settlements.

The sand ridges in the backshore are significantly reworked and mostly covered by scrubs and wild creepers. The River Sundri flows in the south along lush green mangroves. On the road to the fishing jetty, exposures of basalts of different lithology occur such as porphyritic, vesicular, zeolitic and fine grained. These formations perhaps resulted from a series of different lava flows

during the Deccan volcanic event. Lateritic capping is common over these basaltic outcrops. Similar lithology is recorded all along the adjacent coastal areas of Konkan coast as the regional rock types. The regional setup illustrates the rocky coastline trending north-south direction, provided with pocket beaches and bays. Along the Konkan coast of rocky features, depositional landforms are rare but for pocket bays and small beaches. But the study area has slightly a different geomorphology of having enclosed bay surrounded by two promontories and a river in between. This morphological set-up could be one of the reasons for encouraging deposition by the extreme events. As far as the occurrences of extreme events are considered along the Konkan coast. they comparatively few per year unlike in the Bay of Bengal.

### **3.0 Materials and methods**

An automatic level (Trimble) was used to carry out beach profiling, across and along the coast to understand the morphology of the shore. The profile lines share the common transects with that of the GPR survey lines. Two transects near the Sundri River were surveyed (Fig.1b) viz., i) perpendicular (Line L1) to the coast from low tide level to the backshore (~80 m long; west to east) and ii) parallel (Line L2) to the coast on the raised beach ridge (~140 m long; north to south). A GPS (Garmin, with an accuracy of  $\pm 5$  m) was used to obtain the spatial positions of survey and sampling locations.

The SIR-20 GPR system, developed by the GSSI (Geophysical Survey System Inc.), USA was used for GPR profiling. A subsurface profile of 8 m depth penetration (200 ns) was collected using a 200 MHz antenna to get an idea on the general insight of the sub-surface features from the tidal influenced zone to backshore area. In addition, 4 m depth profile (100 ns) was also collected using 400 MHz antenna (better resolution than 200 MHz profile) for the purpose of sedimentary sequence identification. Before the commencement of GPR survey, the radar system was initialized to the field conditions by setting the relevant parameters (such as dielectric constant 15; samples/scan 512; bits/sample 16; scans/sec 100; scan/m 20; gain range 9.0, 35.0, 56.0, 73.0, 76.0; approximate depth range 200 ns (for 8 m depth profile) and 100ns (for 4 m depth profile etc.) in the file header. Some of the parameters (such as, position (ns), meters/mark; scans/mark; dielectric constant etc.) could be editable during post-processing stage. The file header was also edited to include location, surface material characteristic and other useful information in characterizing the survey location. While tuning the system, the measuring wheel also got validated by comparing the horizontal distance in the profile with the field measurements. Proper care was taken to maintaining the optimum antenna towing speed along the profile line. Repeated surveys were carried out to check the consistency of the data. The time domain geo-radar profiles were processed with RADAN

software. The profiles were normalized through low pass filtering for removal of high frequency noises and subsequently, the flat lying ringing system noise was removed by high pass filtering. The deconvolution and migration techniques were carried out to eliminate the ringing multiples and the diffraction respectively in the data. The velocity analysis was performed to estimate the depth or thickness of various sedimentary layers in the profiles. In case of homogeneous and isotropic media, the relative propagation of velocity is calculated from  $v = c \text{ ms}^{-1}$  and the depth derived from  $d = vt \frac{\epsilon_r}{2}$  m; where  $\epsilon_r$  is the relative permeability and  $t$  is the two-way time from the target (Daniels 2007). For a velocity model, parameters such as stacking (improvement in signal to noise ratio), appropriate conversion from travel time into depth and migration are considered. Among many methods to measure the velocity, the analysis of velocity spectra is widely used by the software. The velocity spectrum is generated when stacking results are plotted with velocity versus two-way travel-time as traces or iso-amplitudes.

Further, the data have been enhanced with various digital processing techniques including Hilbert transformation algorithm through which the time domain radar data were transformed in to magnitude and frequency domain data to enhance some of the subtle subsurface features. The transformed information usually displays the significant dielectric changes and variation of some of the features based on respective dielectric constants. The Hilbert transform output articulates the relationship between the magnitude and phase of a signal while the magnitude output specify the raw energy reflected from an object or a layer which would be additionally useful to recognize or to confirm some of the subsurface features.

For verification of the GPR data, two trial pits were made (pit-1 to 100 cm depth and pit-2 to 215 cm depth (Fig. 2b1 and b2) and the sedimentary sequences were recorded. Samples at various depths were collected for granulometric and mineralogical analyses from pit-1. Based on the field sedimentological observations, the samples for OSL dating were collected at night (around 2100 hrs) following the standard procedures of OSL sample collection from pit-2. Two samples from the top and bottom of the pit-2 were collected and subsequently analyzed at the Wadia Institute of Himalayan Geology, Dehradun, India. The data of pit-1 are correlated with the observed GPR profiles.

## 4.0 Results

### 4.1 Observations from field pits

Trial field pit-1 has a top layer (A) of loose fine sands up to 43 cm depth followed by alternatively a mixed coarse and fine sand layers up to ~100 cm depth (Table 1; Figure 2b1). These

alternative sediment classes of fine (moderately sorted) and medium sand (poorly sorted) were coarsely skewed. The sediments are polymodal sediment type. The bi-variant plots of mean  $v/s$  standard deviation, mean  $v/s$  skewness, skewness  $v/s$  kurtosis and skewness  $v/s$  mean have shown the dominance of dune, beach and river environments. This suggests that the contribution of the sediments is from beach and from the Sundri River. Two thin layers of heavy mineral sequences (C and E), dominantly of fine grained ilmenite of 7 and 5 cm thickness respectively, are intervened by a 5 cm layer of pebble (D) at ~60 cm depth and ~100 cm depth. (Fig.2b2).

#### **4.2 OSL dating**

The OSL data of the Palshet sediments indicate that these sediments (130-165 cm depth) were deposited around  $132 \pm 14$  (146 years) years BP i.e., around the year 1866. When this time period is compared with the available data on the history of cyclone in Maharashtra, it suggests that probably the event that occurred is geologically correlated with the recorded severe cyclone event of 1854. According to Murray et al. (2007) the errors in the OSL dates occur due to the sensitivity during the measurement of natural signal, contamination of quartz and open system radionuclide behavior amongst others. Another error is the inaccurate estimation of long term water content which cannot be identified and quantified. Perhaps these errors could account for the marginal error between the reported event date (1854) and the obtained OSL date (1866).

#### **4.3 GPR reflections and core data**

The GPR profile along Line-1 was from the low tide level to the backshore zone. It was ~80 m long with 8 m depth penetration (200 ns velocity range). The time domain GPR profile was normalized with elevation correction using beach profile information and vertically corrected image is presented in Figure 3a. Based on the reflection characteristics, the profile has been discussed here under two segments i.e., i) Zone 1: Foreshore subsurface (0 to 44.0 m stretch) and ii) Zone 2: Backshore subsurface (44.0 to 80.0 m stretch). The zone 1 is characterized with a prominent reflection (higher reflectance and amplitude) in the sub-surface below the high tide level, indicates a buried sand bar feature (Fig. 3a) which was remarkably noticed than the surrounding area. Since the time domain GPR data was processed through the low-pass, high-pass filters, deconvolution and migration techniques to possibly remove high frequency noises, flat lying ringing system noises, ringing multiples and the diffraction respectively, the possibility of reverberations is minimum. Due to difficulty in collecting samples in the inter-tidal zone, the occurrence of this buried sand bar is further analyzed through velocity model (Fig.3 b1) of a selected strip in the profile and are discussed in the section 5.1. From the profile, this buried feature could be observed to extend up to ~6 m depth

and is about 12 m wide. The observation reveals that, in earlier time, this buried sand bar could have been a shallow sand barrier in the nearshore environment. Other than the sand bar feature, the subsurface information of zone 1 is observed to be poor due to high level of saline water saturation condition.

The zone 2 shows water saturation (low amplitude signals) below 2 m depth while in the upper region (surface level to 2 m depth), two types of sand layers (upper and lower) were observed, indicating the progressive deposits in two major spells of times. The observation from the pit-1 (surface to upper layers) indicates the alternative bed sets of fine and medium sorted sediments. Also it is noticed that the fine sand layers are enriched with heavy minerals. These layer information up to 1 m depth is comparable with the GPR reflections (Fig. 3a).

Along Line-2, a 4 m depth profile was generated which was ~140 m long, running parallel to the coast but on the raised beach ridge. The digitally enhanced time domain in grey shades (Fig. 4a) revealed that an erosional surface (bounding surface of consolidated nature) (marked as 1 in the figure) is observed throughout the profile at ~3 m depth. This bounding surface is overlain by a series of sand layers with varied thickness of many sedimentary layer sets. Based on the reflections, 9 different layers were delineated and traced including bounding surface. The core data from the pit-1 could be correlated with the upper layers up to 1 m depth (Fig.3). The entire profile could be discussed as two segments; i.e., i) 10-100 m stretch and ii) 100-140 m stretch. The first stretch of profile has cyclic sedimentation of well sorted and poorly sorted strata as partly supported by the pit-1 (up to 1 m depth) and the second stretch has a series of sedimentary layers with low amplitudes of reflection due to the presence of a finer sand materials than the first one. The change in reflection probably indicates a paleo-channel signature.

## **5.0 Interpretation**

### **5.1 Radar Facies and sedimentary sequences**

In both the profiles, the radar facies representing reflection of various sedimentary strata are evident and could be interpreted with the help of observation from the field pit as well as from the velocity diagram. Since pit can be made up to 1 to 2 m depth depending upon the water table, the velocity diagrams support to characterize the sedimentary layers even below 2 m depth. The velocity diagrams are generated for specific strip of the profile to confirm the changes in the layer sediment sequences at the specific locations.

In the Line-1 profile (Fig.3), the pattern of reflections related to the sedimentary deposition in the foreshore subsurface (zone 1) and the backshore subsurface (zone 2) are quite contrasting,

indicating a different environment of deposition. Since no trench or pit could be opened up in the inter-tidal area due to water saturation and augering problems, a velocity diagram was prepared and shown in Figure 3b1. Due to consolidated nature of the sand bar area, the velocity was more as indicated by the higher value of amplitude traces. The velocity remarkably decreases below down depth. After the high tide area and at the start of berm area, between ~34 to 44 m of the profile, there was an abrupt signal attenuation (very low amplitude) which indicates a high moisture zone. A velocity diagram in this strip further indicates a mixed ranges of velocity in the near subsurface due to high saturation of saline water in the sediments. Such a low reflection points to the deposition of sediments under submerged condition. This zone probably indicates the presence of a paleo-beach environment and is further confirmed by the dipping layers of sand towards the sea afterwards. The sand bar observed in the foreshore subsurface reveals that the sand bar could have been a submerged shoal or sand bar before the shoreline regression due to recent deposition. The backshore subsurface (zone 2) illustrates upper and lower sedimentary layers up to 2.5 m depth. These two sedimentary units are different from each other and their differences were inferred from the changes in velocity (Fig.3 b3) significantly. The lower layer has more compactness than upper one which is loose sandy cover with less moisture. The depth of pit-1 reached up to upper layer boundary, indicating a cyclic deposition of heavy and light mineral layers, in other way, fine and coarse sedimentary layers respectively. The signal attenuation below 2.5 m is attributed to water saturation / high moisture.

While considering the situation of a possible paleo-beach at ~ 34 m, there is a scope to infer the regression of the coast by ~30 to 34 m. This could be possible if there had been a huge deposition of sediment by an extreme event like storms / cyclones. Consequently, the evidence of a huge unrelated pebbly raised beach ridge at the backshore confirmed the above scenario / observation from the GPR profile. The overall inferences from the GPR profile illustrate an uncertain circumstance of high energy deposition which is also duly supported by the physical evidences in the field and sediment sequences observed in the field pit.

From the Line-2 profile (Fig.4a), based on the reflection pattern, 9 sedimentary sequences are recognized from the time domain data (Fig.4a) which further confirmed by the Hilbert magnitude transformed data (Fig. 4b). Since the magnitude transformation from time domain data by Hilbert algorithm indicate the information on raw energy reflected from layers, this techniques was considered here for confirmation. The time domain data in a grey shaded line scan display (Fig. 4a) indicate clearly some of the sub-surface features and significantly, the bottom erosional surface / consolidated layer (1) could be mapped easily. The pattern and structure of bedding are appreciably observed in all the layers. In addition to the information as deduced from the Line-1 profile up to 2.5



m depth (using 200 MHz antenna), the Line-2 profile revealed information up to 4 m depth (using 400 MHz antenna).

While the top surface layer (9) consists of loose sands, the layers 7 and 8 (< 1 m thickness) represents reworked sediments of fine as well as medium grained sands with well sorted and poorly sorted characters respectively. The layers 4, 5 and 6 (0.5 to 2.0 m depth) are each ~1.5 m thick and were deposited by an extreme event as evidenced by the characteristics of sediment sequences from the field pits. Though the field observation could not be done below 2 m depth, the layers 2 and 3 are noticed having similar characteristics of above layers which infers the initial phase of deposition by the extreme events on the erosional base (EB) / bounding base (1) (=lower layer as inferred in Figure 3). This erosional base (below ~2.5 m depth) is compact when compared to overlain deposits as revealed from the velocity diagrams (Fig. 4 c1, c2 and c3). Overall observation indicates that the profiles the Line-1 and Line-2 are comparable as far as the sedimentary bed sets are concerned. Though the nearby Sundri River had tendency to cut through the sediments in the past, eventually, it was forced to shift its course to southerly to attain the present day configuration. This avulsion of the Sundri River is evident in the extreme right part of the profile (Fig. 4a and b) as illustrated by low amplitude traces. The sedimentary sequences a to d (in the right part of the profile) are continuation of 4 to 7, but were cut and filled-in again during the stages earlier to the avulsion of the River. Due to minimum amplitude signals, the paleo-channel zone is well recognized than the surrounding features.

## **6.0 Discussion**

### **6.1 Stages of shifts in river course**

The shifting of river course (avulsion) is a normal development in a river system, i.e., following new course in adjacent areas (Slingerland and Smith 2004). The guidelines for identifying avulsion stratigraphy were outlined by Kraus and Wells (1999) and associated characterization of avulsion deposits was detailed by Jones and Hajek (2007). The changes in river course in historical times (Slowik 2013) and the filling of left-out channel scours or depressions on the bar surface was effectively traced (Smith et al. 2006) using GPR. In the present study area, avulsion caused by extreme-event sedimentation was recognized using GPR and their characteristics are discussed here. While considering the raw energy reflected from various sedimentary sequences, as observed from the magnitude domain GPR data (Fig.4b), other than the surface layers (7,8 and 9), three major units were recognized from the Line-2 profile, i.e., i) the bottom consolidated base / erosional base (x) which was traced easily from its reflection, ii) sediments sequences (2 to 6) deposited over the erosional base (y) and iii) paleo-channel deposits (a to d) which have a prominently low reflection

amplitude than the surrounding areas. Again, the observations evidently revealed the common range of reflection amplitude for layers 2 to 6 which indicated a single time of deposition. Similar observation of various radar facies were identified in the sand south Saskatchewan River, Canada (Smith et al. 2006) using GPR survey. Likewise, Neal et al. (2002) has recognized bounding surface and the intervening bed sets in the mixed-beach deposits at Aldeburgh in Suffolk, south-east England using GPR. The stages of paleo-channel were remarkably traceable due to their characteristic low amplitude reflection.

Based on the figures 4a, and b, a sketch showing the dispositional sequences of various major layers along with the paleo-channel and its progressive shifts are illustrated (Fig. 5). Initially, layer 2 was deposited on the erosional base and followed by the layer 3. During these stages, the river was pushed towards south and the layers 2 and 3 become paleo-banks of the river. One can appreciate that the layers 2 and 3, each about 0.5 to 0.75 m thick indicate their morphological association with the earlier course of the river by their gentle termination towards the riverside. The flat but gently dipping surfaces of layers 2 and 3 substantiates that the river-side features existed in the past while the other layers (4, 5 and 6) were later imprinted with a regular pattern of deposition by an extreme event and were cut by the earlier fluvial process. The continuity of deposition patterns (a with 4; b with 5; c with 6 and d with 8) in the paleo-channel development with the extreme event deposition is evident and comparable. It shows that the fluvial process regulated the sediments when deposited on its course by the extreme event. Once the deposition exceeded the capacity of river action to regulate, the river started migrating towards south. This phenomenon also revealed that the source of sediments was deposited by the extreme event from northern side. Again the paleo-fluvial action in sediment regulation is confirmed by the polymodal characteristic of the sediments as observed from the pit samples.

## **5.2 Development of paleo-channel stages**

The ability of delineating the position of paleo-channels and sedimentary units within, was demonstrated by Gourry et al. (2003). The reflection amplitude of the paleo-channel is very low and indicates a significant loss of signal in this area. When compared to nearby areas, the stages of the paleo-channel are vividly illustrated in the GPR profile and are easily traceable (Fig. 6). It is observed that the paleo-channel runs for about 50 m long and is 2.5 m deep. Interestingly, at every 0.5 m, stages of progression (a, b and c) are observed in consonance with the nearby subsurface layers. This indicates that the river strived to maintain its course at each stage but the sediments spilled over and silted the main course. The other evidence was the presence of paleo-river sand bars (e) in between the paleo-channel area (Fig. 6a, c and d). In the latter stage of extreme even

deposition, the spilled away sediments caused to form river shoals / sand bars, but due to more sediment deposition, the river migrated, allowing in between areas be filled subsequently.

It is further observed that the accumulation of this large deposit of sand could not be possible from a small and sluggish river like Sundri. This suggests that the river traversed through the sand deposited during the 1854 cyclone event. The stages of paleo-channel formation are in consonant with the 1854 cyclone as clearly illustrated by the significant reflection in the time, magnitude and frequency domain GPR data (Fig. 6a, b, c and d). The raw energy reflected from the paleo-channel areas in the form of magnitude information (C) as well as the frequency information (D) is quite evident. The GPR derived spatial information was transferred to the field observation and it was found that the orientation concurrently attest to the existence of paleo-channel with respect to the present day conditions (Fig.7).

### **5.3. Formation of raised beach ridge**

The geomorphology of the partly enclosed Palshet coast shows the occurrence of a raised beach ridge to nearly 4 m from the mean sea-level (Fig. 3 and 7). This observation is corroborated by satellite imagery which also revealed the raised beach ridge (Fig. 8). Hill and promontories composed of basaltic and lateritic rocks enclose a bay where the Sundri River meets the Arabian Sea. The raised beach ridge is located parallel to the coast but perpendicular to the river and the ridge is complemented by a steep beach towards the seaside and vast low lying areas to the landward side. This clearly substantiates our observation of rapid deposition of sediments by an extreme event. Similar situation was reported by Neal et al. (2002) in the mixed sand and gravel beach deposits at Aldeburgh, England and described that the backshore berm ridges owe their source to discrete depositional episode associated to storm-wave activity. Storm dominated progradation with similar nature has been reported in Castle Neck barrier, Massachusetts, USA (Dougherty et al. 2004). In the present study area of Palshet coast, as observed from the field pits, the pebbles and medium to coarser sand with heavy mineral content dominate the sand composition which also indicates their marine origin. Similar observation was reported from the southeast coast of India where alike textural results indicate the source of extreme wave action (Vijayalakshmi et al. 2010). In consonance with the physical criteria set by Morton et al. (2007) and observations by Kortekaas and Dawson (2007) in Martinhal, Portugal, the deposits in the study area (Palshet) own its origin associated with the storm event since they are composed of multiple sub-horizontal planar lamina bed sets and do not contain mud layers or mud intraclasts. Internal structure of the raised beach as revealed by GPR profile consists of various planar bed sets upon bounding surface illustrates a rapid deposition. Studies carried out by Tamura et al. (2008) on raised beach deposits in the Pacific coast

of eastern Japan and Clemmensen and Nielson (2010) on raised beach system in Anhiltn Denmark using GPR also substantiated the present study results.

The coastal geomorphology of the area during before and after the 1854 storm is illustrated in the Figure 9. Before the noted extreme event, the river confluence was open to the bay and sediment were discharged to sea through the bay, causing a development of series of submerged shoals / sand bar due to enclosed and calm condition prevailed in the bay. Due to these submerged shoals, a submerged deltaic feature could have developed. This feature gave raised to the existing marsh land due to inter locked condition, once huge deposits were dumped by the 1854 storm. Since the submerged shoals behaved as main obstacles, the sudden in-flush of huge sediments from the storm were deposited next to submerged shoals, gave raise to elevated beach ridge in multiple series of deposition. During this situation, the river started cut-through operation to reach the sea and finally shifted towards south and found its path as seen today.

As indicated by the results of the GPR data, it was noted that the moisture content present throughout the layers 2 to 6, suggest a predominantly homogeneous source of deposition. Since the fluvial process involving a rain-fed small river had a lesser chance of depositing such huge sediments assorted with pebbles in this area, the other factors like composition of the sediments and orientation of the sediment also do not support the influence of fluvial process. It could be possible to ascertain that the nature of deposition of this raised beach ridge certainly points to various spells of a single episode of deposition and the OSL dating confirms the impact of the 1854 cyclone episode.

## **5.0 Conclusions**

Two GPR profiles viz., one perpendicular to the coast from low tide level to berm (Line-1) and another on the raised beach ridge parallel to the coast (Line-2) of the Palshet coast (Maharashtra, India) were analyzed to map the subsurface features at various depth. The digitally enhanced Line-1 profile revealed the presence of a paleo-beach which is ~34 m from the present coastline (low tide line) and suggests the regression of the coast by ~30 to 34 m. The field evidences indicate that this regression was due to a sand deposit (2.5 m thickness) that forms a raised beach ridge in the backshore area. The GPR profile (Line-2) displays the occurrence of a paleo-channel and the significant presence of massive deposits of sand on the consolidated bounding surface at ~2.5m depth. The study further reiterates that the raised beach sediments were deposited by an extreme event and is perhaps co-relatable with the cyclonic storm that occurred in the area in the year 1854. As a consequence, the progressive deposition of the sediment by the extreme event influenced the Sundri River to shift its course in stages to its present southerly location.

## Acknowledgements

The financial support from the Council of Scientific & Industrial Research, New Delhi through the Network Project (CMM 0023) is gratefully acknowledged. We thank the Directors of CSIR-CIMFR, CSIR-NIO and WIHG for permission to publish this paper. We appreciate the help rendered by Ms. Ruenna D'Souza and Ms. Dashimi Chari for analyzing the samples and secretarial assistance. We are grateful for the comments and suggestions by the reviewers which helped to revise the manuscript. We thank Dr. Gunter Doerhoefer, Editor-in-Chief for encouraging us to submit the revised version of the manuscript. This is NIO's contribution no....

## References

- Altdorff D, Epting J, Kruk J, Dietrich P, Huggenberger P (2013) Delineation of fluvial sediment architecture of subalpine riverine systems using noninvasive hydrogeophysical methods. *Environ Earth Sci* 69 (2): 633-644.
- Clemmensen LB, Nielsen L (2010) Internal architecture of a raised beach ridge system (Anholt, Denmark) resolved by ground-penetrating radar investigations. *Sediment Geol* 223 (3-4):281-290.
- Daniels DJ (2007) *Ground Penetrating Radar*. 2<sup>nd</sup> Edition. The institution of Engineering and Technology, London
- Dougherty A.J, FitzGerald DM, Buynevich IV (2004) Evidences for storm-dominated early progradation of Castle Neck barrier, Massachusetts, USA. *Mar Geol* 210:123-134
- Dube SK, Rao AD, Sinha PC, Murty TS Bahulayan N (1997) Storm surge in the Bay of Bengal and Arabian Sea: The problem and its prediction. *Mausam* 48(2):283-304
- Evan AT, Camargo SJ (2011) A climatology of Arabian sea cyclonic storms. *J Climate* 24(1):140-158
- Gourry J.-Ch, Vermeersch F, Garcin M, Giot D (2003) Contribution of geophysics to the study of alluvial deposits: a case study in the Val d'Avaray area of the river Loire, France. *J Appl Geophys* 54(1-2):35-49. doi: 10.1016/j.jappgeo.2003.07.002
- Jones HL, Hajek EA (2007) Characterizing avulsion stratigraphy in ancient alluvial deposits. *Sediment Geol* 2001(1-2):124-137. doi: 10.1016/j.sedgeo.2007.02.003
- Kortekaas S, Dawson AG (2007) Distinguishing tsunami and storm deposits: An example from Martinhal, SW Portugal. *Sediment Geol* 200:208-221. doi: 10.1016/j.sedgeo.2007.01.004
- Koster B (2012) Ground penetrating radar (GPR) investigations on tsunamigenic deposits: Examples from southern Spain and Greece. *Quatern Int* 279-280(16):254
- Kraus MJ, Wells TM (1999) Recognizing avulsion deposits in the ancient stratigraphical record. In: Smith ND, Rogers J (ed) *Fluvial Sedimentology VI*, Special Publication of the International Association of Sedimentologists 28:251-268

- Loveson VJ, Barnwal RP, Singh VK, Gujar AR Rajamanickam GV (2005) Application of ground penetrating radar in placer mineral exploration for mapping subsurface sand layers: A case study. In: Loveson VJ, Chandrasekar N, Sinha A (ed) Developmental Planning of Placer Minerals. Allied Pub., New Delhi, pp.71-79
- Loveson VJ, Gujar AR (2010) High resolution mapping, modeling and evolution of sub-surface geomorphology using ground penetrating radar techniques: In Anbhazagan S, Subramanian SK, Yang (ed) Applied Geomatics in Geomorphology. Taylor & Francis, pp.119-139
- Loveson VJ, Gujar AR, Barnwal R, Rajamanickam GV (2014) GPR studies over tsunami affected Karaikal beach, Tamil Nadu, South India. *J Earth Syst Sci* (in press)
- Maksim B, Marquis G, Nivière B, Maurin JC, Cushing M (2000) Investigating alluvial and tectonic features with ground-penetrating radar and analyzing diffractions patterns. *J Geophys* 43(1):33-41: doi: 10.1016/S0926-9851(99)00031-2
- Morton RA, Gelfenbaum G, Jaffe BE (2007) Physical criteria for distinguishing sandy tsunami and storm deposits using modern examples. *Sediment Geol* 200 (3–4):184-207
- Murray AS, Svendsen JI, Manqerud J, Astakhoy YI (2007) Testing the accuracy of quartz OSL dating using knowledge Eemian site on the river Sula, northern Russia. *Quat Geochronol* 2:102-109
- Murty TS, El-Sabh MI (1984) Cyclones and storm surges in the Arabian Sea: A brief review. *Deep Sea Research Part A. Oceanographic Research Papers*, 31(6–8): 665-670
- Neal A, Pontee NI, Pye K, Richards J (2002) Internal structure of mixed-sand-and-gravel beach deposits revealed using ground-penetrating radar. *Sedimentology* 49(4):789-804. doi:10.1046/j.1365-3091.2002.00468.x
- Patidar AK, Maurya DM, Thakkar MG, Chamyal LS (2007) Fluvial geomorphology and neotectonic activity based on field and GPR data, Katrol hill range, Kachchh, Western India. *Quatern Intl* 159 (1): 74-92. doi: 10.1016/j.quaint.2006.08.013
- Pedgley DE (2012) Cyclones along the Arabian coast. *Weather*. 24(11):456-470. doi: 10.1002/j.1477-8696.1969.tb03121.x
- Rajeevan M, Srinivasan J, Niranjana Kumar K, Gnanaseelan C, Ali MM (2013) On the epochal variation of intensity of tropical cyclones in the Arabian sea. *Atmospheric Science Letters* 14(4):249-255
- Shukla SB (2012) Ground Penetrating Radar (GPR) studies along the SW Kachchh coast, Western India: Implications in reconstructing high energy event history. *Quatern Int* 279-280(16):447
- Slingerland R, Smith ND.(2004) River avulsions and their deposits. *Annu Rev Earth Pl Sc* 32(1):257-285. doi: 10.1146/annurev.earth.32.101802.120201
- Słowik M (2011) Changes of river bed pattern and traces of anthropogenic intervention: The example of using GPR method (the Obra River, western Poland). *Applied Geography* 31(2):784-799

- Śłowik M (2012) Influence of measurement conditions on depth range and resolution of GPR images: The example of lowland valley alluvial fill (the Odra River, Poland). *Jour Appl Geophys* 85:1-14. doi:10.1016/j.jappgeo.2012.06.007
- Śłowik M (2013) GPR and aerial imageries to identify the recent historical course of the Odra River and spatial extent of Obrzańskie Lake, altered by hydro-technical works. *Environ Earth Sci* doi: 10.1007/s12665-012-2215-9
- Smith GHS, Ashworth P J, Best J L, Lunt I A, Orfeo O, Parsons D R (2009) The Sedimentology and Alluvial Architecture of a Large Braid Bar, Rio Parana, Argentina. *Journal of Sedimentary Research* 79(8) 629-642. doi: 10.2110/jsr.2009.066
- Smith GHS, Ashworth PJ, Best JL, Woodward J, Simpson, CJ (2006) The sedimentology and alluvial architecture of the sandy braided South Saskatchewan River, Canada. *Sedimentology* 53(2) 413-434: doi 10.1111/j.1365-3091.2005.00769.x
- Sridhar A, Patidar A (2005) Ground penetrating radar studies of a point bar in the Mahi River basin, Gujarat. *Curr Sci Ind* 89:183-189
- Tamura T, Murakami F, Nanayama F, Watanabe K, Saito Y (2008) Ground-penetrating radar profiles of Holocene raised-beach deposits in the Kujukuri strand plain, Pacific coast of eastern Japan. *Mar Geol* 248, (1-2):11-27
- Unnikrishnan AS, Kumar M, Ramesh R, Sindhu B (2011) Tropical cyclones in the Bay of Bengal and extreme-sea level projections along the east coast of India in a future climate scenario. *Curr Sci Ind* 101: 327-331
- Vandenbergh J, van Overmeeren R.A, (1999) Ground penetrating radar images of selected fluvial deposits in the Netherlands. *Sediment Geol* 128, 245-270
- Vijaya Lakshmi CS, Srinivasan P, Murthy SGN, Trivedi, D, Nair, R (2010) Granularity and textural analysis as a proxy for extreme wave events in southeast coast of India. *J Earth Sys Sci* 119(3) 297-305. doi:10.1007/s12040-010-0023-8

## Caption to Figures

1. (a) Location map; (b) GPR survey plan at the Palshet beach, Maharashtra, India
  2. (a) Lateritic pebble berm at the Palshet coast; (b1) Sedimentary sequences observed from the field pit-1; (b2) OSL sample site at pit-2. (Legend: A= Surface layer; B= medium sand of light minerals; C= Ilmenite rich heavy mineral layer; D= pebble layer; E= Ilmenite rich heavy mineral layer; F= medium sand of light minerals; G= Heavy minerals at the upper and light minerals and pebbles lower part).
  3. Time domain line scan GPR profile collected using 200 MHz antenna along Line-1 at the Palshet coast.
  4. a) Time b) Magnitude domain GPR profile collected using 400 MHz antenna along Line-2 at the Palshet coast. (1 - 9 signify sedimentary sequences and “a - d” represent stages of paleo-channel development; x) Extreme event deposits; y) Erosional base; z) Paleo-channel; c1, c2 and c3 represent velocity diagram of selected strips (60-62m; 110-112; and 135-137m) from Line-2 profile; EB illustrates Erosional base.
  5. Sketch showing various subsurface features as extracted from the GPR profile collected using 400 MHz antenna along Line-2. ((1 - 9 represent sedimentary sequences and “a - d” illustrate the stages of paleo-channel development.
  6. Reflection signatures of paleo channel stages as deduced from time domain color scan data (A), time domain grey shade scan data (B), Hilbert magnitude domain data (C) and Hilbert frequency domain data (D) (part of Line-2). (a to d represent various paleo channel stages, explained in the text) (data collected using 400 MHz antenna)
  7. Panoramic view of the raised beach ridge and indication of the paleo-channel occurrence.
  8. A Satellite view of the raised beach ridge and location of the paleo-channel of the Palshet coast. (Source: Google maps).
- Figure 9. a) Coastal Geomorphology before extreme event; b) after the extreme event deposition 1. Lateritic capped basaltic headland; 2. River terraces; 3. Alluvial sands; 4. submerged delta; 5. Submerged shoals / sandbars; 6. Marshy land; 7. Raise beach ridge by extreme event deposits.



Table 1. Sediment Characteristics of Pit-1 at the Raised Beach Ridge, Palshet Coast, Maharashtra

Sample Depth (cm)	Median	Mean	Sorting ( $\sigma$ )	Skewness (Sk)	Kurtosis (K)	Sediment Class				Sediment Type	Sediment Name	Heavy Mineral %	Light Minerals %
0-43 A	2.523	2.368	0.844	-0.638	3.781	Fine Sand	Moderately Sorted	Coarse Skewed	Mesokurtic	Polymodal, Moderately Sorted	Moderately Sorted Fine Sand	Top 53.55 Bottom 38.08	Top 46.45 Bottom 61.92
44-52 B	3.030	2.856	0.843	-1.962	9.479	Medium Sand	Poorly Sorted	Coarse Skewed	Leptokurtic	Polymodal, Poorly Sorted	Poorly Sorted Fine Sand	43.27	56.73
53-60 C	2.500	2.351	0.864	-0.435	3.473	Fine Sand	Moderately Sorted	Coarse Skewed	Mesokurtic	Polymodal, Moderately Sorted	Moderately Sorted Fine Sand	50.84	49.16
61-67 D	2.135	1.854	1.107	-0.353	1.390	Medium Sand	Poorly Sorted	Very Coarse Skewed	Leptokurtic	Polymodal, Poorly Sorted	Poorly Sorted Fine Sand	43.30	56.7
68-73 E	2.260	2.200	0.906	-0.858	3.972	Fine Sand	Moderately Sorted	Coarse Skewed	Very Leptokurtic	Polymodal, Moderately Sorted	Moderately Sorted Fine Sand	52.52	47.48
74-80 F	2.103	1.873	1.201	-0.370	2.140	Medium Sand	Poorly Sorted	Very Coarse Skewed	Mesokurtic	Polymodal, Poorly Sorted	Poorly Sorted Fine Sand	37.10	62.9
81-100 G	2.650	2.691	0.651	-0.949	6.706	Fine Sand	Poorly Sorted	Very Coarse Skewed	Very Leptokurtic	Polymodal, Poorly Sorted	Poorly Sorted Fine Sand	Top 66.42 Bottom 37.28	Top 33.58 Bottom 62.72

Legend: A= Surface layer; B= mixed layer with heavy and light sand; C= Ilmenite dominated heavy mineral layer; D= pebble layer; E= Ilmenite dominated heavy mineral layer; F= medium sand dominantely of light minerals; G= Top portion is dominantely by fine heavy minerals and graded down in to sand of light minerals and pebbles dominated.

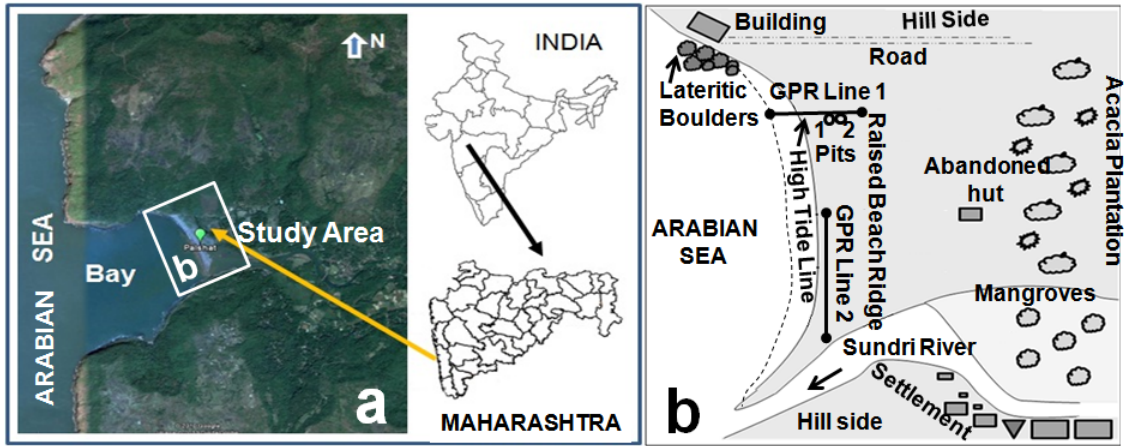


Figure 1.

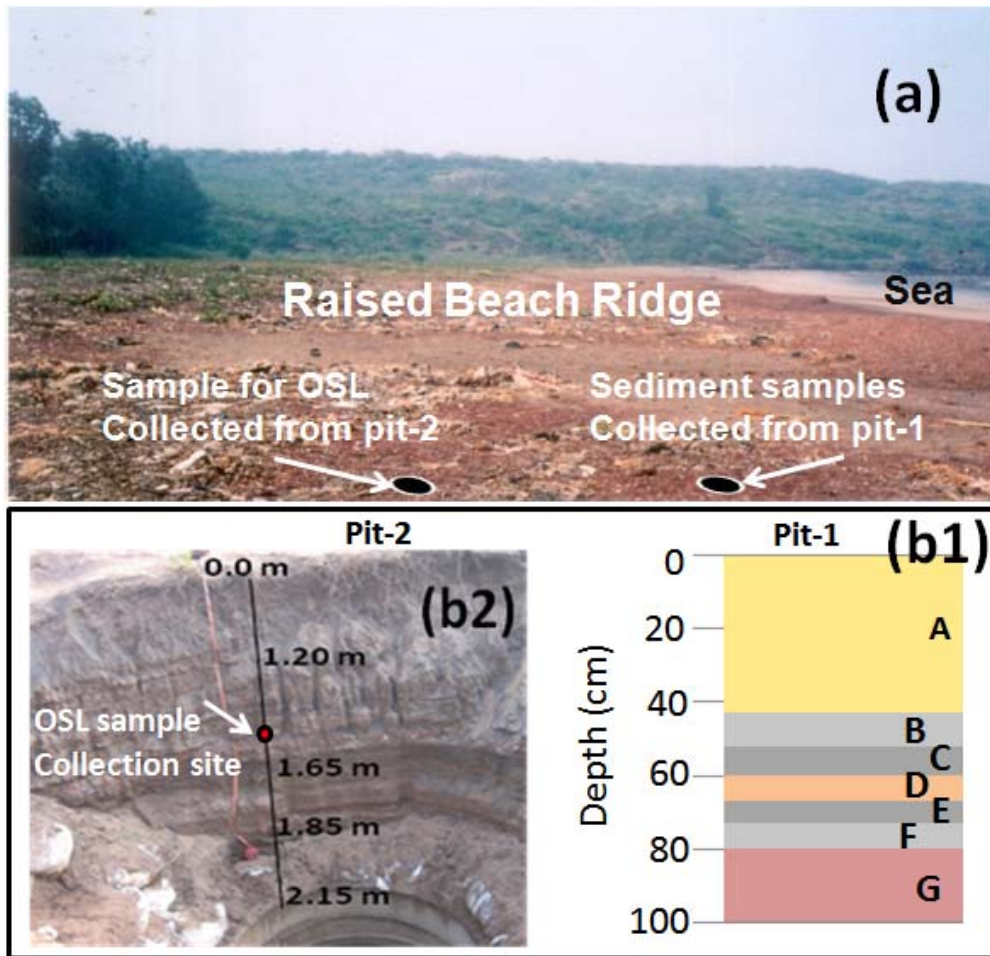


Figure 2.

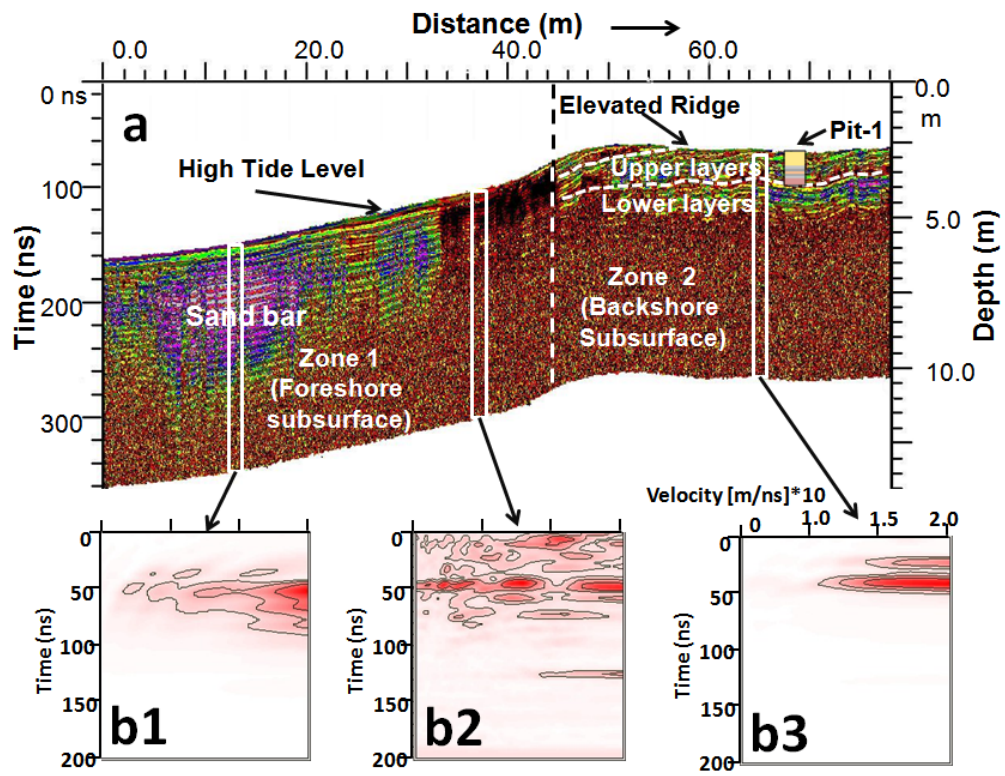


Figure 3.

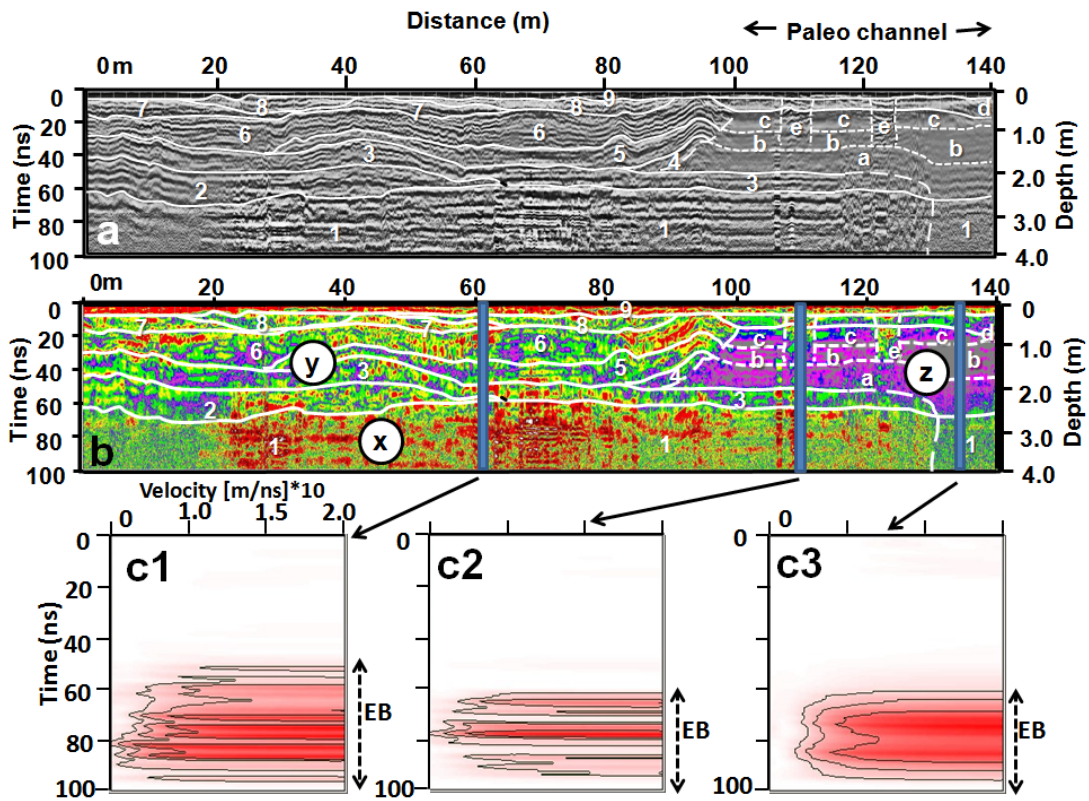


Figure 4.

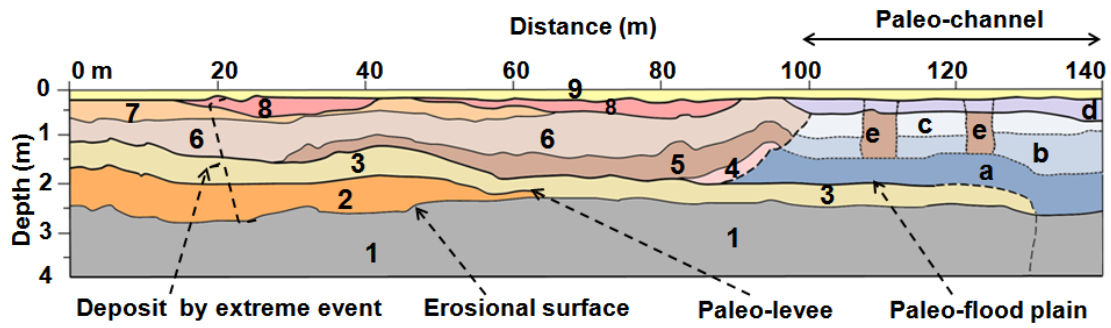


Figure 5.

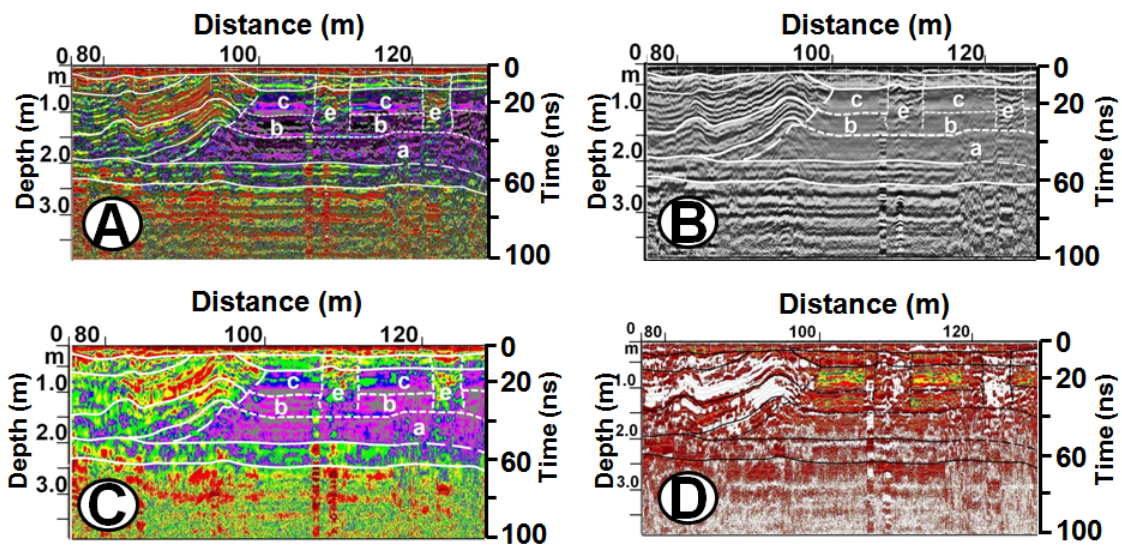


Figure 6.

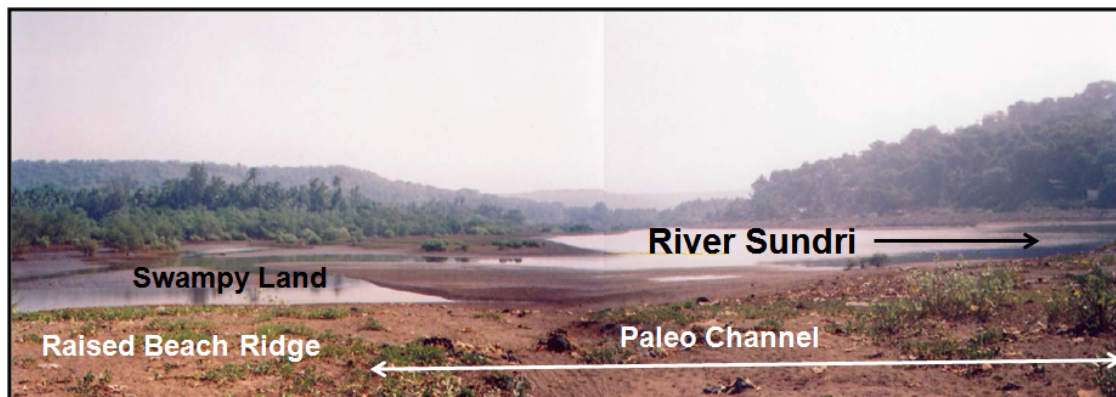


Figure 7.



Figure 8.

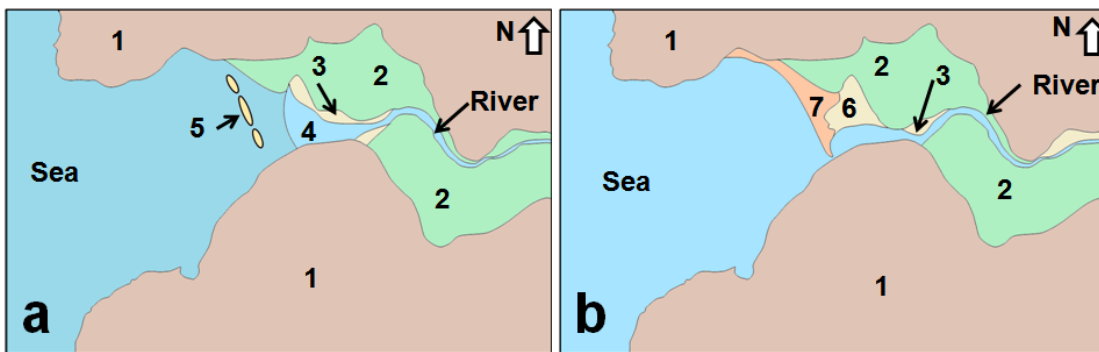


Figure 9.